

Vapor Transport within the Thermal Diffusion Cloud Chamber

Frank T. Ferguson

Department of Chemistry, Catholic University of America, Washington, DC 20064

Richard H. Heist

Department of Chemical Engineering, University of Rochester, Rochester, New York 14627-0166

Joseph A. Nuth, III

Code 691, NASA-Goddard Space Flight Center, Greenbelt, Maryland 20771

A review of the equations used to determine the 1-D vapor transport in the thermal diffusion cloud chamber (TDCC) is presented. These equations closely follow those of the classical Stefan tube problem in which there is transport of a volatile species through a noncondensable, carrier gas. In both cases, the very plausible assumption is made that the background gas is stagnant. Unfortunately, this assumption results in a convective flux which is inconsistent with the momentum and continuity equations for both systems. The approximation permits derivation of an analytical solution for the concentration profile in the Stefan tube, but there is no computational advantage in the case of the TDCC. Furthermore, the degree of supersaturation is a sensitive function of the concentration profile in the TDCC and the stagnant background gas approximation can make a dramatic difference in the calculated supersaturation. In this work, the equations typically used with a TDCC are compared with very general transport equations describing the 1-D diffusion of the volatile species. Whereas no pressure dependence is predicted with the typical equations, a strong pressure dependence is present with the more general equations given in this work. The predicted behavior is consistent with observations in diffusion cloud experiments. It appears that the new equations may account for much of the pressure dependence noted in TDCC experiments, but a comparison between the new equations and previously obtained experimental data are needed for verification.

INTRODUCTION

Prior to the advent of and ready access to inexpensive computers, major advances in our understanding of physical phenomena were often dependent on finding a good approximation to the real-world system where the solution could be computed analytically and was expected to closely match the measured response of the actual physical system. Today, the availability of powerful personal computers makes it easier to solve most, well-defined, bounded transport problems "exactly" via numerical techniques. However, in what follows we will show that problems can sometimes arise when previously derived approximations find their way into such numerical routines rather than using the slightly more complex equations upon which the original approximation was based.

The thermal diffusion cloud chamber (TDCC) has been used to study the nucleation of a variety of materials since its introduction to the nucleation community by Katz and Orstermeir over 30 years ago[1]. In the early years, it was used to measure the critical supersaturation, S_{cr} , the supersaturation at which the flux of droplets was approximately $1 \text{ cm}^{-3}\text{-s}^{-1}$. In the late 1980's as researchers began measuring both the flux as well as the supersaturation, they noticed a dependence of the flux on the background gas that was not seen in typical expansion studies[2]. Since a difference of a few percent in the supersaturation can cause an order of magnitude or more difference in the flux, these flux

measurements were extremely sensitive indicators of differences between the two experimental systems.

To examine the role of the background gas on the nucleation behavior, Heist *et al.* developed a high pressure diffusion cloud chamber (HPCC) capable of studying the nucleation of materials at pressures as high as 40 bar[3-5]. The results of this work seem to suggest that there is a slight pressure dependence of the critical supersaturation, increasing with increasing pressure.

Today there is increasing concern in determining the stable range of operation of the TDCC/HPCC. For example, at sufficiently high pressures, there can be an inversion in the density profile. Such an inversion results in strong convective currents within the chamber, thereby rendering the 1-d model of the TDCC system invalid. A more insidious problem can be caused by convective flows generated by sidewall buoyancy effects. In this case, convective flows can cause a slight, yet systematic change in the temperature and mole fraction profiles within the chamber. Because of their small magnitude, it may be difficult to detect such flows.

To examine the possible magnitudes of these flows, Ferguson and Nuth developed a 2-dimensional model of a typical diffusion cloud chamber which includes the appropriate buoyancy effects[6]. Ferguson and Nuth found that small flows can exist and, for the cases they investigated, these flows were able to reduce the maximum supersaturation along the centerline by roughly 2-8%.

The equations used to solve for the temperature

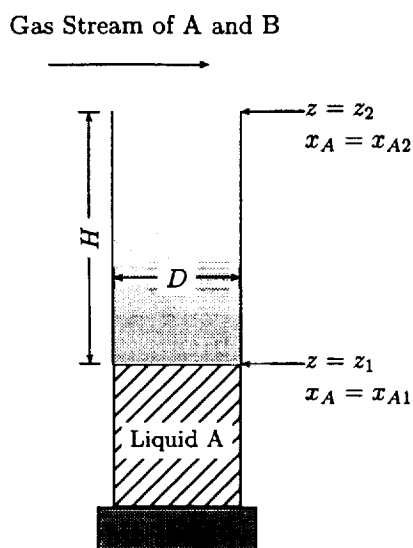


Figure 1— Cross-sectional diagram and mass transfer boundary conditions for the classical Stefan Tube problem.

and concentration fields are coupled and depend upon the expressions used for the physical properties of the constituent species. In order to clearly delineate the effects due to buoyancy alone, the authors calculated the maximum supersaturation within the chamber with the model at a gravitational level of 1 and 0. With $g=0$, buoyancy effects are eliminated and the results should be identical to the typical 1-d modeling (provided the diameter to height ration (D/H) is sufficiently high and the wall effects do not extend to the centerline).

Although very close, the 0g solutions and that of the typical 1-d modeling did not match identically, even using identical physical properties. The following discussion outlines the differences between these two approaches and the source for this discrepancy.

MODELING OF THE TDCC

The development of the equations for the TDCC follow very closely those for the classical Stefan tube problem as outlined by Bird, Stewart and Lightfoot[7]. Such an apparatus can be used to measure binary diffusion coefficients and a diagram of a typical Stefan tube apparatus is shown in Figure 1. The tube is filled with a liquid A evaporating into a background gas B and it is assumed that the mole fraction at the liquid surface is given by the ratio of the equilibrium vapor pressure at the temperature of the liquid to the total pressure. At the top of the tube, the mole fraction of A is also specified.

Fick's law for the transport of A is

$$N_A - x_A(N_A + N_B) = -cD_{AB}\nabla x_A \quad (1)$$

where N_i is the molar flux of species i with respect to a fixed coordinate system, c the molar concentration of the mixture, D_{AB} the binary diffusion coefficient and x_i

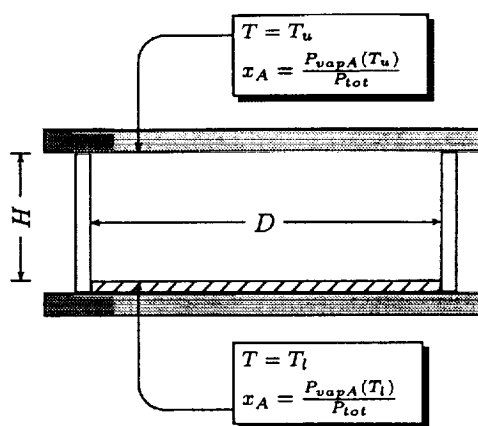


Figure 2— Typical thermal diffusion cloud chamber and transport boundary conditions.

the mole fraction of species i . If we assume the flux is 1-dimensional and that the background gas is essentially stagnant, (i.e. $N_{Bz} = 0$) we get

$$N_{Az} = -\frac{cD_{AB}}{1-x_A} \frac{dx_A}{dz} \quad (2)$$

If it is assumed that the tube is at steady state and isothermal and that the gases behave ideally, a shell balance for the flux of A can be used to develop analytical expressions for the mole fraction profile and the rate of evaporation[7].

A diagram of a typical diffusion cloud chamber and the boundary conditions for the typical 1-d modeling are shown in Figure 2. The TDCC differs from the Stefan tube in that the top boundary is closed and the bottom and top surfaces are held at different temperatures. During operation, vapor diffuses from the hotter, lower plate towards the cooler, upper plate. At sufficiently high supersaturations the vapor condenses and forms droplets which fall back to the lower plate. In order to model the system in 1-dimension only, the D/H ratio of such chambers are typically large, approximately 5 or greater. In contrast, Stefan tubes typically have very low D/H ratios to minimize end effects (e.g. error in fluid meniscus level, circulating flows at the top of the tube).

Katz originally developed the equations describing transport in the TDCC[8]. Because the system is not isothermal, an additional equation is needed for the temperature profile. The mass flux in the 1-d system is given by

$$x_B N_{Az} - x_A N_{Bz} = -cD_{AB} \left[\frac{dx_A}{dz} + k_T \frac{d}{dz} \ln T \right] \quad (3)$$

where k_T is the thermal diffusion coefficient and T the temperature. The second term in the brackets accounts for the influence of the temperature field on the mass flux, i.e. the Soret effect. Again the assumption is made that the flux of B is zero; hence the equation can be written as:

$$x_B N_{Az} = -cD_{AB} \left[\frac{dx_A}{dz} + k_T \frac{d}{dz} \ln T \right] \quad (4)$$

It is more convenient to define the thermal diffusion ratio, α , as

$$\alpha = \frac{k_T}{x_A x_B} \quad (5)$$

Also, the following substitution can be made for the mole fraction, x_A ,

$$x_A = \frac{P}{P_t} \quad (6)$$

where P is the partial pressure of A and P_t is the total pressure within the chamber. The binary diffusion coefficient, D_{AB} , can be expressed as

$$D_{AB} = \frac{D_{AB}^0 T^s}{c} = \frac{D_{AB}^0 R T^{s+1}}{P_t} \quad (7)$$

where D_{AB}^0 is a constant and s is a factor ranging from 0.5 to 1.0. Substituting these expressions into equation (4) yields a differential equation for the partial pressure profile of A :

$$\frac{dP}{dz} = \frac{\alpha P(P - P_t)}{T P_t} \frac{dT}{dz} + \frac{(P - P_t)L}{T^s D_{AB}^0} \quad (8)$$

The heat flux, Q , in the TDCC consists of three terms: transport by conduction, transport due to convective flux, and the Dufour effect. This flux is given by

$$Q = -k \frac{dT}{dZ} + N_{Az} H + \frac{RT k_T N_{Az}}{x_A} \quad (9)$$

where k and H are the thermal conductivity and enthalpy of the mixture, respectively. Using the same substitutions as used for the molar flux equation gives

$$\frac{dT}{dZ} = \frac{1}{k} \left[-Q + N_A \left(H + \frac{\alpha RT(P_t - P)}{P_t} \right) \right] \quad (10)$$

The coupled differential equations, (8) and (10), can be solved numerically for the temperature and partial pressure profile to determine the supersaturation profile. The approach is straightforward and very plausible, yet there are some inconsistencies when one considers the momentum equation governing the system.

INCONSISTENCIES IN THE MODELING

Inside the TDCC, in the absence of any buoyancy-induced convection, there should be no mass average velocity, \mathbf{v} , within the chamber. For a justification of this statement we look at the momentum equation for this steady system:

$$\nabla \rho \mathbf{v} \cdot \mathbf{v} = -\nabla P + \mu \nabla^2 \mathbf{v} + \rho \mathbf{g} \quad (11)$$

In this equation, \mathbf{v} is the mass average velocity, ρ , the density, P , the pressure, μ , the fluid viscosity, and \mathbf{g} , the gravitational acceleration. In equation (11), the only sources for momentum generation are the pressure gradient term, ∇P , and the body force term, $\rho \mathbf{g}$. Since there are no pressure gradients within the chamber (essentially isobaric and closed) and buoyancy forces are neglected

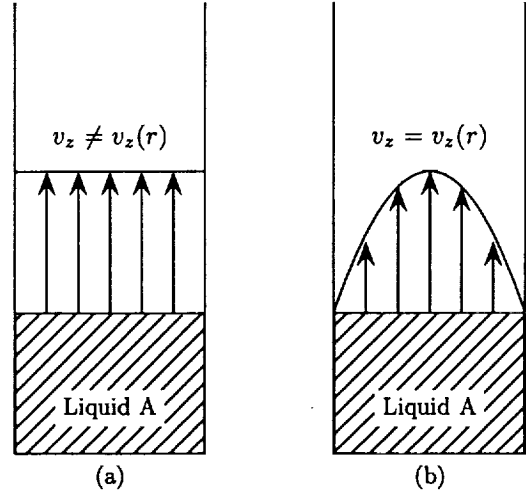


Figure 3— Two different concepts of the velocity profile within the stefan tube and diffusion cloud chamber.

(which is consistent with the assumptions of 1-d transport in the chamber), the momentum equation becomes

$$\nabla \rho \mathbf{v} \cdot \mathbf{v} = -\mu \nabla^2 \mathbf{v} \quad (12)$$

Since there are no moving boundaries or velocity components at the boundaries, we are left with the trivial conclusion that the mass average velocity, \mathbf{v} , is zero everywhere within the chamber. Furthermore, the continuity equation for this 1-d, steady system is

$$\frac{d\rho v_z}{dz} = 0 \quad (13)$$

which implies that the $\rho v_z = \text{constant}$. Again, since the velocities at the boundaries equal zero it follows that the velocity must be zero everywhere within the chamber.

Yet, as Whitaker points out, the equations given in (2) and (4) suggest that there is a convective flux present[9]. For example, the mass average velocity in the system is given by

$$\mathbf{v} = \frac{1}{\rho} [\rho_A \mathbf{v}_A + \rho_B \mathbf{v}_B] \quad (14)$$

since $\rho_i = c_i M_i$ where M_i is the molecular weight of species i and $\mathbf{N}_i = c_i \mathbf{v}_i$ we have

$$\mathbf{v} = \frac{1}{\rho} [N_A M_A + N_B M_B] \quad (15)$$

or in 1-dimension

$$v_z = \frac{1}{\rho} [N_{Az} M_A + N_{Bz} M_B] \quad (16)$$

but it has been assumed that $N_{Bz} = 0$; therefore,

$$v_z = \frac{1}{\rho} [N_{Az} M_A] \quad (17)$$

which contradicts the conclusions derived from both the momentum and continuity equations. Furthermore, there is no radial dependence in this equation for the velocity in the chamber and this equation predicts a flat velocity profile as shown in Figure 3-(A); yet such a profile violates the no-slip boundary condition at the chamber side wall. The no-slip boundary at the chamber sidewall should give a parabolic-type of velocity profile as shown in Figure 3-(B).

Finally, the ordinary, concentration-induced molar flux of A for both the Stefan tube and the TDCC are given by equation (2). Whitaker also notes that this equation for the flux suffers from problems as $x_A \rightarrow 1.0$ [9].

There appears to be considerable confusion in the literature regarding the transport of vapor in the Stefan tube and these same problems appear in the equations used to describe the TDCC. These problems arise from the assumption that the background gas, B , is stagnant. In a 1-d system, for reasons mentioned earlier there should not be any mass-averaged velocities in a Stefan tube or TDCC.

It was recognized quite a while ago that the uniform velocity profile violated the no-slip boundary condition at the wall. It was assumed that there was some radial variation in the concentration gradient. Heinzelmann *et al.*[10] performed a detailed experimental and theoretical analysis of the Stefan tube assuming no-slip at the walls and concluded that the radial concentration was essentially uniform within their experimental error[10]. Rao and Bennet[11] performed another study of radial concentration effects in the Stefan tube and arrived at a similar conclusion.

Later on, justifications for the apparent discrepancy between the velocity profile of species A and the no-slip boundary condition came including the existence of a recirculating flow in the tube[12] and the presence of slip at the walls. Kramers and Kistemaker[13] postulated the existence of a diffusive slip boundary condition in the presence of a concentration gradient and this was invoked by Whitaker as a possible explanation for the momentum boundary condition inconsistency[14]. Unfortunately, Kramers and Kistemaker made a mistake in the reference frame upon which they based their theoretical treatment of slip. This error gives a nonzero velocity or slip effect at the walls which is not actually present[15]

Markham and Rosenberger[16] performed a full numerical simulation of the Stefan tube which did not include the assumption of a stagnant background gas and imposed the no-slip boundary condition. Unfortunately, the assumption of a bulk velocity associated with the Stefan tube is so entrenched in the literature that they *specified* a velocity at the liquid surface based on equation (2) which is, in turn, based on the stagnant B approximation. By specifying a velocity at the surface, they, *by necessity*, found a recirculating flow which was influenced by the gravitational level. In their work the authors note that they were left with a singularity in

the corners of their solution domain where the specified velocity at the liquid surface met the no-slip boundary condition of the tube walls. It is interesting to note that in their analysis there was considerable recirculation of the background gas, B .

In the case of the Stefan tube there is an advantage to making the assumption that the background gas is stagnant. Using this assumption, the differential equation describing the vapor transport in the Stefan tube can be solved analytically to yield reasonable estimates of the vapor concentration profile and flux. Since the TDCC is not isothermal, the equations describing the energy and mass transport in the TDCC are coupled and must be solved numerically. Therefore, there is no significant computational advantage to making the stagnant gas assumption in this case.

STAGNANT GAS ASSUMPTION

In this section we examine the effect of the assumption that the background, carrier gas is stagnant. For simplicity, we neglect the cross-coupling terms in the transport equations. The emphasis of this analysis is to highlight the differences between the terms describing ordinary, concentration-induced diffusion; the cross-coupling terms would unnecessarily complicate the analysis and may be included in a full analysis with little effort.

A mass balance on species A , at steady state and without generation terms through chemical reactions gives

$$\nabla \cdot (\rho \omega_A \mathbf{v}) = (\nabla \cdot \rho D_{AB} \nabla \omega_A) \quad (18)$$

where ω_A is the mass fraction of species, A . Since the velocities in the momentum and continuity equations are mass average velocities, there is an advantage to switching to mass fractions for concentrations rather than using mole fractions. In equation (18), for 1-d without any flow ($\mathbf{v} = 0$ everywhere) based on the previous justifications, the inertial term drops out and we are left with

$$\frac{d}{dz} \left[\rho D_{AB} \frac{d\omega_A}{dz} \right] = 0 \quad (19)$$

Had we used an equivalent equation for the molar concentration we would be left with a convective term dependent upon the non-zero, molar average velocity. The mass average velocity must satisfy the typical, hydrodynamic boundary condition of no-slip at the walls, but there is no such restriction on the molar average velocity. Therefore it is possible to have a convective flux using molar units, even though there might not be a convective flux while using mass units.

Using $\rho = cM$ where M is the mean molecular weight of the mixture and

$$\omega_A = \left[\frac{x_A M_A}{M} \right] \quad (20)$$

in equation (19) gives

$$\frac{d}{dz} \left[\frac{c D_{AB} M_A M_B}{M} \frac{dx_A}{dz} \right] = 0 \quad (21)$$

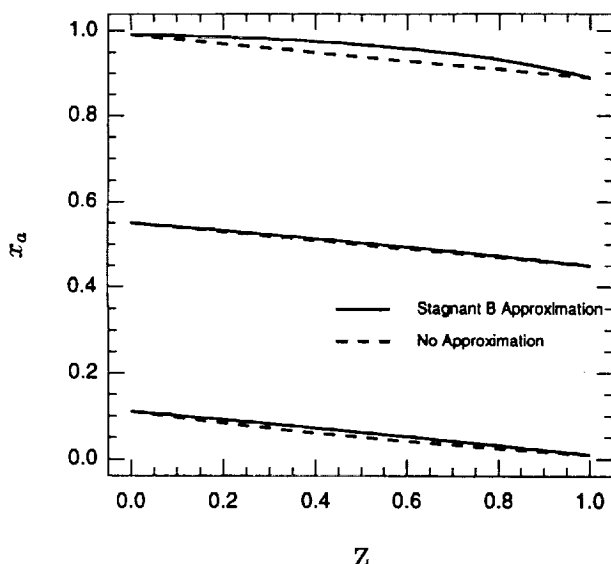


Figure 4— A comparison between the predicted mole fraction profiles based on the stagnant gas assumption and no assumption about the background gas. Curves are shown for different concentrations with a total Δx_A of 0.1.

and since M_A and M_B are constants

$$\frac{d}{dz} \left[\frac{cD_{AB}}{M_B + (M_A - M_B)x_A} \frac{dx_A}{dz} \right] = 0. \quad (22)$$

This equation should be compared with the equation under the stagnant gas approximation,

$$\frac{d}{dz} \left[\frac{cD_{AB}}{(1 - x_A)} \frac{dx_A}{dz} \right] = 0 \quad (23)$$

As $x_A \rightarrow 0$, the denominator of equation (22) $\rightarrow M_B$. Since the denominator of equation (22) is just the mean molecular weight of the binary mixture, it is always greater than zero.

COMPARISON BETWEEN EXPRESSIONS

What is the difference in the mole fraction profiles between equations (22) and (23)? To examine this effect we assume that the cD_{AB} product is a constant, (which is reasonable for an ideal gas mixture); then the equations reduce to a comparison of

$$\frac{d}{dz} \left[\frac{1}{(1 - x_A)} \frac{dx_A}{dz} \right] = 0 \quad (24)$$

and

$$\frac{d}{dz} \left[\frac{1}{M_B + (M_A - M_B)x_A} \frac{dx_A}{dz} \right] = 0 \quad (25)$$

For the second equation we need molecular weights so we choose $M_A = 60.096$ and $M_B = 4.0026$ corresponding to 1-propanol and helium, respectively, as a test case.

Figure 4 is a comparison between these two equations for 3 different cases with constant difference in the mole fraction at the boundaries, Δx_A , of 0.1. The resulting profiles will depend upon the value of x_A so three

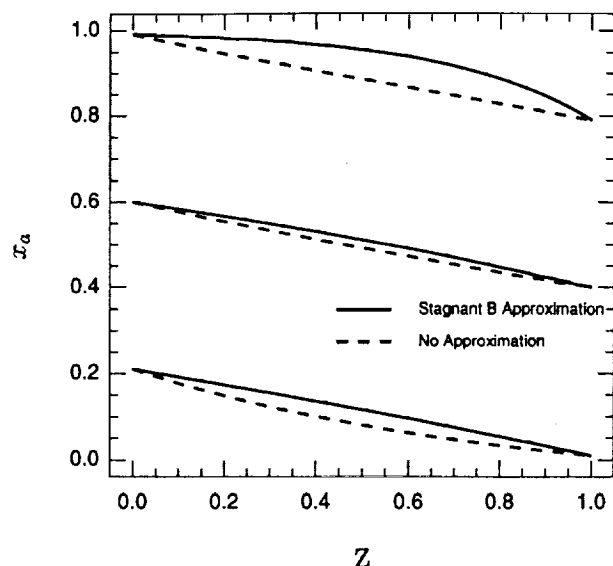


Figure 5— A comparison between the predicted mole fraction profiles based on the stagnant gas assumption and no assumption about the background gas. Curves are shown for different concentrations with a total Δx_A of 0.2.

extreme cases are shown in the graph; $x_A \rightarrow 0$, $x_A \sim 0.5$, and $x_A \rightarrow 1.0$. The dark curve denotes the typical, stagnant background gas solution while the dashed curve is the profile calculated without this approximation.

In all three cases, equation (25) predicts a smaller value for the mole fraction than equation (24). For values of $x_A \sim 0.5$, there is virtually no difference between the two solutions. As $x_A \rightarrow 0$ and $x_A \rightarrow 1.0$, the differences between the two profiles are larger and the effect is more pronounced for the $x_A \rightarrow 1.0$ case.

Figure 5 is a similar plot for the mole fraction profile, but with a larger concentration difference between the boundaries. In this case, the concentration difference between the two boundary points is 0.2. Again, in all cases the stagnant background gas approximation predicts a higher value for the mole fraction of A at any point over the results from equation (25).

The differences between the two profiles are again the smallest for the $x_A \sim 0.5$ solution, but the differences between the solutions are more dramatic for the $\Delta x_A = 0.2$ case than the $\Delta x_A = 0.1$ case.

Because of the coupling between the equations for the concentration and temperature profiles, it can be hazardous to draw general conclusions as to the results on the supersaturation profile. The results from Figures 4 and 5 seem to suggest that the supersaturation calculated via equation (25) will always be lower than that calculated using equation (24) and these differences will be more pronounced as the concentration of the vapor becomes very small or very large.

CALCULATION OF SUPERSATURATION DATA

To examine the effect of the stagnant background gas approximation on the actual supersaturations calculated, we will examine two test cases. The first of these

Expt. No.	S_{max}	S_{max}	S_{max}
Soret/Dufour Effects Included?	Yes	No	No
$N_{Bz} = 0$ Assumed?	Yes	Yes	No
Source of Data?	Katz[8]	This Work	This Work
6	13.46	13.61	6.43
6 ^a	13.72	13.36	7.51
11	26.54	26.92	11.59
15	41.89	42.08	17.88
15 ^a	41.5	40.12	21.3

Table 1— Comparison between maximum supersaturation values for nonane taken from the work of Katz[8] (column 2), calculated using the stagnant gas assumption (column 3), and calculated without the stagnant gas assumption (column 4). Experiments highlighted with an ^a represent runs where the total pressure in the chamber was doubled.

will be the condensation of 1-propanol in helium at 1.18 bar with lower and upper plate temperatures of 302.9 and 256.5 K, respectively. The maximum supersaturation between the two plates is calculated via the typical 1-d equations derived by Katz and by the following two equations for the temperature and mass fraction profile, respectively:

$$\frac{d}{dz} \left[k \frac{dT}{dz} \right] = 0 \quad (26)$$

$$\frac{d}{dz} \left[\rho D_{AB} \frac{d\omega_A}{dz} \right] = 0 \quad (27)$$

As with the traditional equations for the TDCC, the condensation flux is assumed to be sufficiently small that effect of the condensing vapor does not significantly influence the temperature or concentration profile as calculated by these equations. Physical properties for both sets of equations were identical and were taken from the tabulated data given by Heist[3]. In both sets of equations the Soret and Dufour effects were neglected and the ideal gas equation of state was used.

The results were an S_{max} of 3.226 calculated via equations (26) and (27) and an S_{max} of 3.66 as calculated via the typical, stagnant background gas solutions. The $S_{max} = 3.226$ is identical to the solution derived by Ferguson and Nuth's 2-dimensional model at 0g[6] while the 3.66 value is close to the value estimated from the graph in the work Bertelsmann and Heist[17]. As expected, the value calculated from the full equations is lower than the stagnant background gas equations and in this case there is just over 10% difference between the two values.

A second comparison is made between the values calculated by Katz for a nonane-helium system[8]. In this case, a direct comparison is more complicated because Katz included the Soret/Dufour effects on the profiles. Fortunately, Katz also included a detailed sensitivity analysis for these same data and examined the effect of several parameters upon the maximum calculated supersaturation anywhere within the chamber. His analysis indicates that the effect of neglecting these coupling

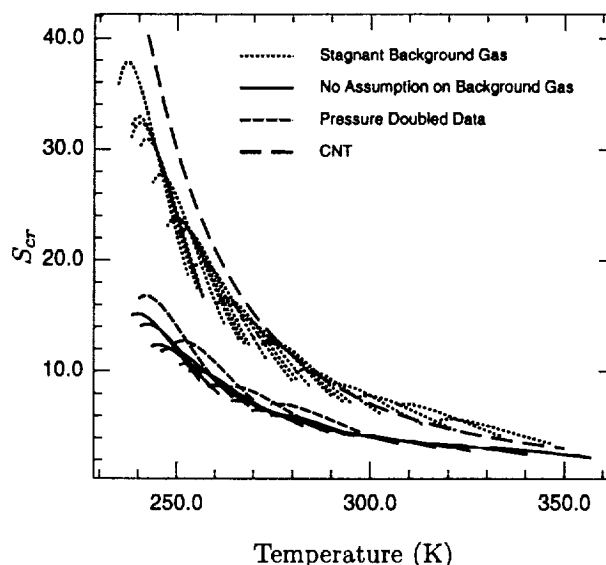


Figure 6— A comparison between nonane experimental data and CNT predictions. The supersaturation prediction from the equations with no assumption on the background gas transport indicate a pressure effect while the typical equations used to calculate the supersaturation profile in the TDCC do not show this effect.

terms causes an approximately 3% deviation in the maximum supersaturation.

Table 1 is a comparison between the values derived by Katz, the values calculated via the stagnant background gas approximation (without Soret/Dufour terms) and the S_{max} calculated without the stagnant background gas approximation. As is seen in the table, the results calculated via our stagnant gas model are consistent with a 3% variation in the values presented by Katz. This reinforces the fact that the physical properties and solution procedure are consistent with those used by Katz. The values for the supersaturation calculated without the stagnant background gas approximation are much lower; approximately 50% lower for most of the cases shown. However, there is a very real concern as to the reliability of all the low temperature critical supersaturation data for nonane (see below).

Katz obtained excellent agreement between the ex-

perimentally measured critical supersaturations (using the equations based on the stagnant gas approximation) for nonane and CNT so discrepancies between these new equations and CNT are likely based on the sample of results in Table 1. The S_{cr} vs. T envelopes from Katz' experimental data are plotted in Figure 6 as short dashes along with the predictions of CNT using the physical properties for nonane given in the original work. As shown in the figure, the agreement between the two is excellent. The experimental data lie a bit below CNT predictions at the lower temperature end and a bit higher at the higher temperature end—this behavior is similar to that seen with a large number of other materials in the TDCC. It is important to point out that all of the supersaturation versus temperature curves shown in Figure 6, except for the five curves in each set at the highest temperatures, violate the stability criteria for stable (e.g. free from buoyancy-driven convective flows) TDCC operation as defined by Bertelsmann and Heist.[17] As a result, all these data are suspect and should most probably be represented by smaller computed supersaturation values.[6,17] However, the reduction in the computed supersaturation due to the buoyancy-driven flow in this case is not as significant as the reduction in the computed supersaturation arising from the stagnant background gas assumption discussed here.

The S_{cr} vs. T envelopes based on the general equations where the stagnant gas assumption is not made are shown as the solid curves. These data fall well below the CNT predictions. At the lower temperature end, the S_{cr} values are less than 1/2 of those of the Katz and CNT predictions and the differences between the two become smaller at the higher temperatures. Another important point to notice is that the data with the stagnant background gas yields a smooth S_{cr} vs. T envelope. In contrast, there are four data sets for the newly calculated data which are markedly higher than the rest of the data set. These four sets correspond to runs where the pressure in the TDCC was doubled.

As noted in the introduction, one of the problems currently plaguing TDCC work is the apparent dependence of the results upon the pressure of the chamber carrier gas. Such an effect is not predicted by CNT or the typical equations used to calculate the supersaturation profile in the chamber. Yet the new transport equations in this work do predict such a rise in supersaturation with increasing pressure.

Again, we restrict our discussion to concentration-induced diffusion and ignore the smaller-order, cross-coupling terms in the mass and energy equations. In this work we have tried to show that equation (19) is consistent with the momentum equation while equation (23), the one typically used in TDCC studies is not. Both equations are of the form

$$\frac{d}{dz} \left[\Gamma \frac{d\phi}{dz} \right] = 0 \quad (28)$$

When steady conditions are reached in the TDCC, the

temperature of the upper and lower plates fix the partial pressure at these boundaries via the vapor pressure equation. These partial pressures are essentially invariant with pressure, so the ϕ 's in equation (28), whether they are mass or mole fractions scale accordingly with pressure—they are both simply different ways of describing the partial pressure profile in the chamber. Variations in the partial pressure *profile* occur between these two fixed boundary conditions because of the factor, Γ , in equation (28). For equation (23),

$$\Gamma = \left(\frac{cD_{AB}}{1 - x_A} \right) \quad (29)$$

The mole fractions in TDCC experiments are typically small. For example, the largest mole fraction of any of the examples shown in Table 1 is 0.15. Therefore, the denominator in equation (29) is ~ 1.0 . Further, the product of cD_{AB} is essentially pressure independent. Hence, a doubling of pressure would make little difference to the supersaturation profile calculated using equation (24).

On the other hand, in equation (19),

$$\Gamma = \rho D_{AB}. \quad (30)$$

In this case a doubling of the pressure effectively doubles this value, thereby altering the calculated supersaturation profile. Equation (27) predicts an increase in the supersaturation with pressure as is typically observed.

As a brief aside, we note that equation (29) will become large as the mole fraction of the diffusing component approaches unity. The region in the TDCC where this will occur is in the vicinity of the lower plate boundary, and the reason why this would occur is operating the cloud chamber under low total pressure conditions. As mentioned earlier, typical values for mole fractions at the lower plate are usually small (several tenths or less), so this is normally not an issue. However, operation under conditions in which the value of the vapor pressure of the diffusing component at the lower plate approaches the magnitude of the total pressure is becoming increasingly important as the cloud chamber is being used to investigate broader classes of working fluids over wider ranges of operational conditions (e.g. nucleation near a critical point[18]).

In experiments, as the value of x_A approaches unity the value of the mass flux will increase significantly and the conditions at the lower plate surface will move increasingly away from equilibrium. When that happens, we are no longer able to use the equilibrium boundary condition approximation for the mole fractions at the lower (and upper) plate surfaces, and we are no longer able to calculate conditions within the chamber. Again, this is generally not a problem as long as the ratio of the mass flux through the chamber to the equilibrium evaporation flux at the lower plate is small. For example, in recent experiments involving pentanol and hydrogen in which operation at low total pressures was specifically investigated, this ratio was typically on the order

of 10^{-6} (even at the lower total pressures used in those experiments[19]).

In the past investigators have relied on empirical rules of thumb to help determine proper operating ranges for the TDCC. One such rule involves the so-called pressure ratio. This quantity is defined as the ratio of the total pressure to the equilibrium vapor pressure of the diffusing material at the lower plate. It is generally accepted that the value of this ratio should be larger than (roughly) two to three and the bigger the better[20]. At first glance it might seem reasonable to associate the effect of the denominator in equation (29) with this pressure ratio.

However, results from the pentanol-hydrogen investigation mentioned above clearly identified a lower total pressure stability limit for diffusion cloud chamber operation below which the nucleation data are increasingly unreliable[19]. In that investigation, mole fraction and temperature profiles within the cloud chamber were determined using the stagnant background gas assumption (including thermal diffusion cross coupling terms and using a real gas equation of state). And, in that investigation, the ratio of the mass flux to the equilibrium flux was generally of the order 10^{-6} . Based on the results of that investigation, it does not appear that the observed limit of lower total pressure stability reported in the pentanol-hydrogen investigation is a consequence of the denominator in equation (29). Rather, as the authors point out, it appears to be associated with the onset of buoyancy-driven convective instabilities within the cloud chamber and appears also to be related to the presence of the thin pool of liquid (source of diffusing vapor) on the lower plate. One other important result of that investigation is that the pressure ratio bears no relation to the lower total pressure limit of stability and should not be used to specify operational conditions for diffusion cloud chamber operation.

CONCLUSIONS

In this work we have tried to highlight a problem in the typical equations used to calculate the supersaturation in the thermal diffusion cloud chamber. As in the classical Stefan tube, this problem seems to arise from the assumption that the background, carrier gas is stagnant. This assumption seems very plausible and intuitive—at first glance it seems to be an accurate assessment of what is occurring in the chamber. The assumption was also crucial in the derivation of an analytical

solution for the Stefan tube system. Unfortunately, the assumption of a stagnant carrier gas manifests itself as a convective flux of the volatile species which is inconsistent with the momentum and continuity equations.

A different equation for the concentration-induced diffusion of the volatile species in the TDCC has been introduced which is consistent with the momentum equation. It is perhaps better to view this approach as regarding the TDCC as a two-point boundary value problem (where the concentration and temperature are specified) and solving for the profiles within the chamber using reasonably general transport equations. Although it appears that these new equations may resolve much of the carrier gas problem in the TDCC in a rather simple fashion, a full test of this approach with experimental data is needed. Fortunately, most of the previously measured experimental data can be easily recalculated.

REFERENCES

- [1] J.L. Katz and B.J. Ostermier, *J. Chem. Phys.* **47** 478, (1967).
- [2] Y. Viisanen, R. Strey, and H. Reiss, *J. Chem. Phys.*, **99**, 4680, (1993).
- [3] R. H. Heist, M. Janjua, and J. Ahmed, *J. Phys. Chem.* **98**, 4443 (1994).
- [4] R. H. Heist, J. Ahmed, and M. Janjua, *J. Phys. Chem.* **99**, 375 (1995).
- [5] R. H. Heist, *J. Phys. Chem.*, **99**, 16792, (1995).
- [6] F.T. Ferguson and J.A. Nuth, III, *J. Phys. Chem.*, **111**, 8013, (1999).
- [7] R. B. Bird, W. E. Stewart, E. N. Lightfoot, *Transport Phenomena*, John Wiley and Sons, New York, (1960).
- [8] J.L. Katz, *J. Chem. Phys.*, **52**, 4733, (1970).
- [9] S. Whitaker, *Ind. Eng. Chem. Res.*, **30**, 978, (1991).
- [10] F.J. Heinzelmann, D.T. Wasan, C.R. Wilke, *Ind. & Eng. Chem. Fundamentals*, **4**, 55, (1965).
- [11] S.S. Rao and C.O. Bennett, *Ind. Eng. Chem. Res.*, **5**, 573, (1966).
- [12] S.S. Rao and C.O. Bennett, *Ind. Eng. Chem. Fund.*, **6**, 477, (1967).
- [13] H.A. Kramers and J. Kistemaker, *Physica*, **10**, 699, (1943).
- [14] S. Whitaker, *Ind. Eng. Chem. Fund.*, **6**, 476, (1967).
- [15] F.T. Ferguson, *Phys. Fluids*, (2000) submitted.
- [16] B.L. Markham and F. Rosenberger, *Chem. Eng. Communications*, **5**, 287, (1980).
- [17] A. Bertelsmann and R. H. Heist, *J. Chem. Phys.* **106**, 610 (1997).
- [18] A. Bertelsmann, P. Ye, and R.H. Heist, *J. Phy. Chem.*, (2000) submitted
- [19] R.H. Heist, A. Bertelsmann, D. Martinez, and Y.F. Chan, *J. Chem. Phys.*, (2000) submitted.
- [20] J.L. Katz, C.J. Scoopa II, N.G. Kumar, P. Mirabel, *J. Chem. Phys.*, **62**, 448, (1975).